

# A comparison of different cluster mass estimates: consistency or discrepancy ?

Xiang-Ping Wu<sup>1,2</sup>, Tzihong Chiueh<sup>1</sup>, Li-Zhi Fang<sup>3</sup> and Yan-Jie Xue<sup>2</sup>

<sup>1</sup>*Institute of Astronomy, National Central University, Chung-Li 32054, Taiwan*

<sup>2</sup>*Beijing Astronomical Observatory, Chinese Academy of Sciences, Beijing 100012, China*

<sup>3</sup>*Department of Physics, University of Arizona, Tucson, AZ 85721, U.S.A.*

submitted 1998 April; accepted 1998 August

## ABSTRACT

Rich and massive clusters of galaxies at intermediate redshift are capable of magnifying and distorting the images of background galaxies. A comparison of different mass estimators among these clusters can provide useful information about the distribution and composition of cluster matter and their dynamical evolution. Using a hitherto largest sample of lensing clusters drawn from literature, we compare the gravitating masses of clusters derived from the strong/weak gravitational lensing phenomena, from the X-ray measurements based on the assumption of hydrostatic equilibrium, and from the conventional isothermal sphere model for the dark matter profile characterized by the velocity dispersion and core radius of galaxy distributions in clusters. While there is an excellent agreement between the weak lensing, X-ray and isothermal sphere model determined cluster masses, these methods are likely to underestimate the gravitating masses enclosed within the central cores of clusters by a factor of 2–4 as compared with the strong lensing results. Such a mass discrepancy has probably arisen from the inappropriate applications of the weak lensing technique and the hydrostatic equilibrium hypothesis to the central regions of clusters as well as an unreasonably large core radius for both luminous and dark matter profiles. Nevertheless, it is pointed out that these cluster mass estimators may be safely applied on scales greater than the core sizes. Namely, the overall clusters of galaxies at intermediate redshift can still be regarded as the dynamically relaxed systems, in which the velocity dispersion of galaxies and the temperature of X-ray emitting gas are good indicators of the underlying gravitational potentials of clusters.

**Key words:** dark matter – galaxies: clusters: general – gravitational lensing – X-rays: galaxies

## 1 INTRODUCTION

Clusters of galaxies are the largest coherent and gravitationally bound objects in the universe. They are often used for cosmological test of theories of structure formation. In particular, their matter composition, the mass-to-light ratio  $M/L$  (e.g. Bahcall, Lubin, & Dorman 1995) and the baryon fraction  $f_b$  (e.g. White et al, 1993) play a potentially important role in the direct measurement of mean mass density of the universe,  $\Omega_m$ . It appears that the observational and theoretical results are likely to merge nowadays, in favor of a low mass density universe of  $\Omega_m \sim 0.3$  (e.g. Bahcall et al. 1995; Ostriker & Steinhardt 1995). Yet, the key issue in such a “direct” measurement of the cosmological density parameter is closely connected to the question of how accurately one can determine the total gravitating masses of galaxy clusters.

Recall that the traditional cluster estimators strongly rely upon the assumption of hydrostatic equilibrium: both optical galaxies and intracluster diffuse gas quasi-statically trace the underlying gravitational potential of the whole cluster. However, a number of recent X-ray observations (e.g. Henry & Briel 1995; Markevitch 1996; etc.) have argued that the hydrostatic hypothesis is inapplicable to at least merging clusters. Therefore, an independent method of estimating cluster mass is highly appreciated. At present, it is widely recognized that the gravitational lensing is a unique and also ideal tool to fulfill the task, in the sense that it provides a fair estimate of cluster masses regardless of the cluster matter components and their dynamical states.

In the framework of gravitational lensing, mapping the gravitational potential of a galaxy cluster can be achieved by the detailed modeling of the strongly distorted and mag-

nified arclike images inside the core of the cluster (Fort & Mellier 1994), by the statistical analysis of the weakly distorted images of faint and distant galaxies around the cluster (Kaiser & Squires 1993), and by counting the populations of distant galaxies (Wu & Hammer 1995; Taylor et al. 1998) and quasars (Wu & Fang 1996a; references therein) around the cluster. A combination of these lensing phenomena would, in principle, allow one to depict an overall matter distribution of cluster on scales spanning two decades from the inner core of  $\sim 30$  kpc to the outer regime of  $\sim 10$  Mpc (Wu & Fang 1996b). However, in the practical measurements the lensing signals often appear to be relatively weak, and a precise determination of cluster masses suffers from the limitations of instrument sensitivities and viewing fields. In particular, for different lensing phenomena different techniques have been developed and employed in the reconstruction of matter distributions of clusters. Hence, before one proceeds to the cosmological applications of the gravitating masses of clusters derived from gravitational lensing, it is also worthy of examining whether different approaches based on different lensing phenomena yield a consistent gravitating mass of cluster.

On the other hand, apart from the doubt as to whether the gravitational lensing provides an accurate cluster mass estimate, it is of great interest to compare the cluster masses derived from traditional method with those from gravitational lensing. Previous comparison has been made among many individual clusters, in which both strongly/weakly distorted images of background galaxies and X-ray/optical emissions are detected. Basically, a good agreement between the X-ray and weak lensing determined cluster masses has been detected (Squires et al. 1996, 1997b; Smail et al. 1997; Allen 1998), in contrast to the situation of strong lensing, in which the lensing derived cluster masses are typically  $\sim 2-4$  times larger than the cluster dynamical masses obtained under the assumption of hydrostatic equilibrium (e.g. Wu 1994; Miralda-Escudé & Babul 1995; Allen, Fabian, & Kneib 1996; Markevitch 1997). This argument is further strengthened by Wu & Fang (1997) using a large sample of 29 lensing clusters drawn from literature. Several attempts have correspondingly been made to explain the discrepancy such as the possible contributions of nonthermal pressure (Loeb & Mao 1994; Ensslin et al. 1997) and projection effect (Miralda-Escudé & Babul 1995; Girardi et al. 1997b). An important progress in understanding the issue has been made recently by Allen (1998), based on a detailed comparison of the cluster mass determinations from X-ray and gravitational lensing for 13 lensing clusters. He showed that the mass discrepancy between the X-ray and strong lensing analyses exists only in the non-cooling flow clusters, which can be well accounted for by the significant offsets between the X-ray and strong lensing centers. This implies that in the central regions of these clusters, the traditional “quasi-static” hypothesis for the X-ray emitting gas has probably broken down. However, it should be noticed that even for these non-cooling clusters the weak lensing determined cluster masses agree nicely with the X-ray determined ones.

The current comparisons of different cluster mass estimates seem to suggest that the reported mass discrepancy between X-ray and gravitational lensing analyses may, at least partially, arise from the employments of different lensing techniques: Strong lensing and weak lensing yield an in-

consistent cluster mass. Although this disagreement could be attributed to observations because strong lensing and weak lensing measurements probe the different regions of clusters, a direct comparison between cluster masses obtained from these two lensing phenomena has now become possible with the progress of weak lensing technique and the increasing population of arcs/arclets. If the cluster masses derived from strong lensing do systematically exceed the weak lensing values, one would be faced with the following difficulties: The consistency of the weak lensing and X-ray determined cluster masses indicates that the strong lensing analysis may lead to an overestimate of gravitating mass for cluster, which requires a re-examination of the modeling of arcs/arclets as the cluster mass estimator. On the other hand, the strong lensing phenomena (arcs or arclets) are usually believed to be a good indicator of the underlying gravitational potential of the lensing clusters, in which there are almost no free parameters once the redshifts of the arclike images are known. This leads us to the possibility that both weak lensing and X-ray measurements may underestimate the true cluster mass by a factor of 2–4. The latter point is directly related to the question whether the previously estimated  $M/L$  and  $f_b$  of clusters gives rise to an underestimate of the cosmological density parameter  $\Omega_m$ . Of course, there may exist a third possibility that enables us to reconcile the cluster mass difference while maintain the validity of these different mass estimators. Alternatively, an examination of the consistency or discrepancy between the strong/weak lensing and X-ray/optical mass measurements of clusters will be of great help to our understanding of dynamical and evolutionary properties of rich clusters at intermediate redshifts. Throughout this paper, we assume  $H_0 = 50 \text{ km s}^{-1} \text{ Mpc}^{-1}$  and  $\Omega_0 = 1$ .

## 2 SAMPLE

By searching the literature, we have collected a strong lensing cluster sample of 38 clusters (Table 1), which contains 48 arc/arclet images of distant galaxies. We adopt only the published data sets of the projected cluster masses within the positions of arcs/arclets and make no attempt as far as possible to extrapolate the original work. Therefore, a number of fainter and smaller arclets have not been included in Table 1. Our weak lensing cluster sample consists of 24 clusters, in which the projected radial mass distributions have been given for 10 clusters while only one mass measurement interior to a certain radius is listed for the remaining clusters. It is helpful to recall how the cluster mass is computed in the framework of gravitational lensing. In the case of strong lensing, the projected cluster mass within the position of arc/arclet  $r_{arc}$  is often estimated through

$$m_{lens,arc}(r < r_{arc}) = \pi r_{arc}^2 \Sigma_{crit}, \quad (1)$$

where  $\Sigma_{crit} = (c^2/4\pi G)(D_s/D_d D_{ds})$  is the critical surface mass density, with  $D_d$ ,  $D_s$  and  $D_{ds}$  being the angular diameter distances to the cluster, to the background galaxy, and from the cluster to the galaxy, respectively. Eq.(1) is actually the lensing equation for a cluster lens of spherical mass distribution with a negligible small alignment parameter for the distant galaxy as compared with  $r_{arc}$ . As for weak lensing, a similar expression to eq.(1) is applied:

**Table 1.** Strong Lensing Cluster Sample

cluster	$z_{cluster}$	$T$ (keV)	$\sigma_{gal}$ (km s $^{-1}$ )	$z_{arc}$	$r_{arc}$ (Mpc)	$mass(10^{14}M_{\odot})$
A370	0.373	$7.1^{+1.0}_{-0.8}$	$1367^{+310}_{-184}$	1.3	0.35	13.0
				0.724	0.16	2.90
A963	0.206	$6.8^{+0.4}_{-0.5}$	$1100^{+480}_{-210}$	...	0.0517	0.25
				0.711	0.080	0.60
A1204	0.170	$3.8^{+0.2}_{-0.2}$	...	...	0.0311	0.10
A1689	0.181	$9.0^{+0.4}_{-0.3}$	$1989^{+245}_{-245}$	...	0.183	3.6
A1835	0.252	$8.2^{+0.5}_{-0.5}$	...	...	0.150	1.98
A1942	0.224	...	...	...	0.0372	0.18
A2104	0.155	...	...	...	0.025	0.064
A2163	0.203	$13.9^{+0.7}_{-0.5}$	1680	0.728	0.0661	0.41
A2218	0.171	$7.0^{+1.0}_{-1.0}$	$1405^{+163}_{-145}$	1.034	0.26	2.7
				0.702	0.0794	0.623
				2.515	0.0848	0.570
A2219	0.228	$11.8^{+1.3}_{-0.8}$	...	...	0.079	0.517
				...	0.110	1.60
A2280	0.326	...	$948^{+516}_{-285}$	...	0.080	0.59
A2390	0.228	$8.9^{+1.0}_{-0.8}$	$1093^{+61}_{-61}$	0.913	0.177	2.54
A2397	0.224	...	...	...	0.0698	0.45
A2744	0.308	$12.1^{+1.4}_{-1.0}$	$1950^{+334}_{-334}$	...	0.1196	1.136
A3408	0.0419	...	...	0.0728	0.0568	0.44
S295	0.299	...	907	...	0.0329	0.14
				0.930	0.14	1.6
CL0024	0.391	...	$1339^{+233}_{-233}$	1.390	0.214	3.324
CL0302	0.423	...	1100	...	0.122	1.60
CL0500	0.327	$7.2^{+3.7}_{-1.8}$	$1152^{+214}_{-214}$	...	0.15	1.90
CL2236	0.552	...	...	1.116	0.0876	0.30
CL2244	0.328	$6.5^{+1.8}_{-1.3}$	...	2.236	0.0465	0.20
MS0440	0.197	$5.3^{+1.3}_{-0.8}$	$606^{+62}_{-62}$	0.530	0.089	0.89
MS0451	0.539	$10.2^{+1.5}_{-1.3}$	$1371^{+105}_{-105}$	...	0.190	5.2
MS0955	0.145	...	...	...	0.0385	0.22
MS1006	0.261	...	$906^{+101}_{-101}$	...	0.079	0.57
				...	0.14	1.8
				...	0.28	7.2
MS1008	0.306	$7.3^{+2.5}_{-1.5}$	$1054^{+107}_{-107}$	...	0.26	6.1
MS1137	0.783	...	...	...	0.044	0.19
				...	0.147	2.1
				...	0.151	2.2
MS1358	0.329	$6.5^{+0.7}_{-0.6}$	$937^{+54}_{-54}$	4.92	0.121	0.827
MS1445	0.257	$5.6^{+0.2}_{-0.3}$	$1133^{+140}_{-140}$	...	0.098	0.86
MS1621	0.427	...	$793^{+55}_{-55}$	...	0.046	0.24
MS1910	0.246	...	...	...	0.33	9.6
MS2053	0.523	...	...	...	0.119	2.60
MS2137	0.313	$4.4^{+0.4}_{-0.4}$	960	...	0.0874	0.71
MS2318	0.130	5.1	...	...	0.12	1.3
AC114	0.310	$8.1^{+1.0}_{-0.9}$	$1649^{+220}_{-220}$	0.639	0.35	13.0
GHO2154	0.320	...	...	0.721	0.0342	0.20
PKS0745	0.103	$8.5^{+1.6}_{-1.2}$	...	0.433	0.0459	0.30
RXJ 1347	0.451	$11.4^{+1.1}_{-1.0}$	1235	...	0.24	4.2

Data are collected from Wu & Hammer (1993), Le Fevre et al. (1994), Kneib & Soucail (1995), Wu & Fang (1997), Allen (1998), Campusano, Kneib & Hardy (1998), Tyson, Kochanski & Dell'Antonio (1998) and Clowe et al. (1998)

**Table 2.** Weak Lensing Cluster Sample

cluster	$z_{cluster}$	$T$ (keV)	$\sigma_{gal}$ (km s $^{-1}$ )	$r$ (Mpc)	$mass(10^{14}M_{\odot})$	references
A1689	0.1810	$9.0^{+0.4}_{-0.3}$	$1989^{+245}_{-245}$	0.20–1.6	3.2–14	Tyson et al. (1995)
A2163	0.2030	$13.9^{+0.7}_{-0.5}$	1680	0.09–0.89	0.34–4.05	Squires et al. (1997b)
A2218	0.1710	$7.0^{+1.0}_{-1.0}$	$1405^{+163}_{-145}$	0.8	$7.8^{+1.4}_{-1.4}$	Kneib et al. (1995)
				0.405	$2.10^{+0.38}_{-0.38}$	Smail et al. (1997)
				0.25–1.16	1.37–11.7	Squires et al. (1996a)
A2263	0.208	...	...	0.87	$5.0^{+2.5}_{-2.5}$	Allen (1998)
A2390	0.2279	$8.9^{+1.0}_{-0.8}$	$1093^{+61}_{-61}$	0.19–1.20	1.59–19.1	Squires et al. (1996)
				0.94	$10^{+4}_{-4}$	Allen (1998)
A2744	0.308	$12.1^{+1.4}_{-1.0}$	$1950^{+334}_{-334}$	0.40	$3.70^{+0.64}_{-0.64}$	Smail et al. (1997)
0957+561	0.36	...	$715^{+130}_{-130}$	0.06–0.80	0.12–1.5	Fischer et al. (1997a)
3C324	1.206	...	...	0.5	6.0	Smail et al. (1995)
3C295	0.46	12.6	$1670^{+364}_{-364}$	0.40	$4.70^{+0.76}_{-0.76}$	Smail et al. (1997)
3C336	...	...	...	0.50	$4.8^{+1.0}_{-1.0}$	Bower et al. (1997)
AC114	0.3100	...	$1649^{+220}_{-220}$	0.50	$4.0^{+0.4}_{-0.4}$	Allen (1998)
CL0016	0.5545	$8.0^{+1.0}_{-1.0}$	$1234^{+128}_{-128}$	0.40	$3.74^{+1.28}_{-1.28}$	Smail et al. (1997)
CL0024	0.3910	...	$1339^{+233}_{-233}$	3.0	40	Bonnet et al. (1994)
				0.40	$2.76^{+0.74}_{-0.74}$	Smail et al. (1997)
CL0054	0.56	...	...	0.40	$3.42^{+1.28}_{-1.28}$	Smail et al. (1997)
CL0303	0.0349	...	$1079^{+235}_{-235}$	0.40	$0.44^{+0.90}_{-0.90}$	Smail et al. (1997)
CL0412	0.51	...	...	0.40	$0.50^{+0.82}_{-0.50}$	Smail et al. (1997)
CL0939	0.4510	$6.7^{+1.7}_{-1.7}$	$1081^{+194}_{-194}$	0.75	$6^{+1}_{-1}$	Seitz et al. (1996)
				0.40	$1.46^{+0.82}_{-0.82}$	Smail et al. (1997)
CL1601	0.54	...	1166	0.40	$1.54^{+1.32}_{-1.32}$	Smail et al. (1997)
MS1054	0.826	$14.7^{+4.6}_{-3.5}$	$1643^{+806}_{-343}$	0.23–2.0	0.62–27.3	Luppino et al. (1997)
MS1137	0.783	...	...	0.18–1.21	1.60–4.74	Clowe et al. (1998)
MS1224	0.3255	$4.3^{+1.15}_{-1.0}$	$802^{+90}_{-90}$	0.96	7.0	Fahlman et al. (1994)
MS1358	0.3290	$6.5^{+0.7}_{-0.6}$	$937^{+54}_{-54}$	0.12–1.29	0.38–3.65	Hoekstra et al. (1998)
RXJ1347	0.4510	$11.4^{+1.1}_{-1.0}$	1235	0.24–2.6	2.6–30	Fischer et al. (1997b)
RXJ1716	0.813	$6.7^{+2.0}_{-2.0}$	1892	0.18–1.11	0.95–5.90	Clowe et al. (1998)

$$m_{lens,weak}(r < r_0) = \pi r_0^2 \zeta(r_0) \Sigma_{crit}. \quad (2)$$

Here  $\zeta$  is defined as (Fahlman et al. 1994)

$$\begin{aligned} \zeta(r_0) &= 2 \left(1 - r_0^2/r_{max}^2\right)^{-1} \int_{r_0}^{r_{max}} \langle \gamma_T \rangle d \ln r \\ &= \bar{\sigma}(r < r_0) - \bar{\sigma}(r_0 < r < r_{max}), \end{aligned} \quad (3)$$

in which  $\langle \gamma_T \rangle$  is the mean tangential shear around a circular path of radius  $r$  introduced by the gravitational potential of the cluster,  $\bar{\sigma}(r < r_0)$  and  $\bar{\sigma}(r_0 < r < r_{max})$  represent the mean surface mass density interior to  $r_0$  and in the annulus  $r_0 < r < r_{max}$ , respectively. Therefore, eq.(2) provides a low bound on the projected cluster mass within  $r_0$ .

In order to reconstruct the cluster mass  $m_{lens,arc}(r < r_{arc})$  or  $m_{lens,weak}(r < r_0)$ , one needs also to know the redshift of the arc/arclet or the spatial distribution of background galaxies. Spectroscopic measurements have been made for about  $\sim 2/5$  of the arcs/arclets in Table 1. When the data of redshifts are not available, a redshift of  $z_s = 0.8$  is often used in the estimate of  $\Sigma_{crit}$ , except for the arcs in clusters MS1137+66 at  $z = 0.783$  where  $z_s = 1.5$  is adopted in Table 1. Such an assumption is justified by the recent

work of Ebbels et al. (1998), who obtained the spectroscopic identifications of 18 arclike images behind A2218 and found a mean redshift of  $\langle z_s \rangle = 0.8-1$  at  $R \sim 25.5$ . Nevertheless, placing the background galaxies at  $z_s = 2$  instead of  $z_s = 0.8$  would reduce the value of  $\Sigma_{crit}$  by a factor of only 1.4 for a mean cluster redshift of  $\langle z_d \rangle \approx 0.3$ . Weak lensing measurements involve a great number of faint and distant galaxies behind foreground clusters, and the spectroscopic measurements of all the population of galaxies in the fields seem to be impossible at present. Different calibrations have thus been applied by different authors in the determinations of  $\Sigma_{crit}$ . For clusters at relatively lower redshifts of  $z_d \approx 0.3$ , it appears to be plausible to assume the mean redshift of the background galaxies to be at  $z_s \sim 0.8-1.2$  when combined with the existing work of deep galaxy surveys. However, it should be noted that the big uncertainty of up to a factor of  $\sim 5$  arising from the unknown redshift distributions of background galaxies may occur in the evaluation of  $\Sigma_{crit}$  for high- $z$  clusters at  $z_d \approx 0.8$  (e.g. Luppino & Kaiser 1997).

Before we turn to the comparison of strong lensing, weak lensing and X-ray/optical determined cluster masses,

we display in Fig.1 the relationship between the velocity dispersion ( $\sigma_{gal}$ ) of galaxies and the temperature ( $T$ ) of X-ray emitting gas for 20 lensing clusters in Table 1 and Table 2, for which both  $\sigma_{gal}$  and  $T$  are available in literature. It is believed that the  $\sigma_{gal} - T$  relationship can provide a straightforward yet robust test for the dynamical properties of clusters of galaxies (Cavaliere & Fusco-Femiano 1976). Employing the least-square fit of a power-law to the data of Fig.1 yields  $(\sigma_{gal}/\text{km s}^{-1}) = 10^{2.57 \pm 0.13} (kT/\text{keV})^{0.59 \pm 0.14}$ . Regardless of its large error bars, this relationship is essentially identical with the one for the nearby clusters (Girardi et al. 1996 and references therein), and is also consistent with the isothermal hydrostatic scenario of  $\sigma_{gal} \sim T^{0.5}$ . Based on the  $\sigma_{gal} - T$  relationship alone, we may conclude that no significant dynamical and cosmic evolution has been detected for those massive lensing clusters within intermediate redshift  $\langle z_d \rangle \approx 0.3$ . It is interesting to recall that similar conclusions have been reached by numerous recent studies on X-ray clusters. For instances, the cluster number counts exhibit no evolutionary tendency at least to redshift of as high as  $z \sim 0.8$  (Rosati et al. 1998), and no significant differences in the X-ray luminosity-temperature relationship and the velocity dispersion-temperature relationship between low-redshift and high-redshift clusters are seen (e.g. Mushotzky & Scharf 1997). In particular, the distribution of core radius of the intracluster gas of nearby clusters accords with that of distant clusters ( $z > 0.4$ ) (Vikhlinin et al. 1998). So, these arguments may eventually support the hypothesis that overall, both galaxies and gas are the tracers of the depth and shape of the underlying gravitational potential of cluster, in despite of the presence of substructures and merging activities on small scales.

### 3 COMPARISONS OF DIFFERENT MASS ESTIMATES

#### 3.1 Strong and weak lensing

Ten weak lensing clusters in Table 2 also contain arclike images of background galaxies in their central cores. Comparison of strong and weak lensing determined cluster masses among these clusters are straightforward and shown in Fig.2. Except for A1689 where the absolute mass calibration was made using the giant arcs which trace the Einstein radius (Tyson & Fischer 1995), the rest strong lensing events seem to yield larger cluster masses than the weak lensing measurements when the two methods become to be comparable with each other at the central regimes. In Fig.3 we display the strong/weak lensing determined cluster masses at different radii utilizing all the data sets in Table 1 and Table 2. Although such a comparison sounds less serious in the sense that they are different clusters, it is by no means of physical insignificance. Indeed, the majority of clusters of galaxies that are capable of magnifying and distorting the images of background galaxies are very rich clusters at intermediate redshift. They are representative of the (most) massive clusters at  $\langle z \rangle \sim 0.3$ . Statistically, their gross dynamical properties should look very similar. It is remarkable that the data points in Fig.3 are clearly separated into two parties: the strong lensing determined cluster masses systematically and significantly exceed the weak lensing values. Actually, the

strong lensing data appear in the plot as if they were the upper limits to the weak lensing measurements. Alternatively, the cluster masses given by the arcs/arcllets with and without confirmed redshifts show no significant differences. The very small dispersion in the strong lensing results arises from the fact that the critical surface mass density parameter  $\Sigma_{crit}$  remains roughly unchanged for the known lensing systems which have a mean cluster redshift of  $\langle z_d \rangle \approx 0.3$  and a mean source redshift of  $\langle z_s \rangle \approx 0.8$ . Consequently, the ‘‘mass density profile’’ derived from the strong lensing events varies as  $r^{-2}$ .

#### 3.2 Lensing and X-ray measurements

X-ray observations have been made for most of the lensing clusters. Under the assumption that the hot diffuse gas is in hydrostatic equilibrium with the underlying gravitational potentials of clusters, one can easily obtain the X-ray cluster masses provided that the gas and temperature radial profiles are well determined. Adopting the conventional isothermal  $\beta$  model for gas distribution which is characterized by the core radius  $r_{xray,c}$ , the index  $\beta_{fit}$  and the temperature  $T$ , we can write out the projected X-ray cluster mass within radius  $r$  to be (Wu 1994)

$$m_{xray} = 1.13 \times 10^{13} \beta_{fit} \tilde{m}(r) \left( \frac{r_{xray,c}}{0.1 \text{ Mpc}} \right) \left( \frac{kT}{1 \text{ keV}} \right) M_{\odot}, \quad (4)$$

where

$$\tilde{m}(r) = \frac{(R/r_{xray,c})^3}{(R/r_{xray,c})^2 + 1} - \int_{r/r_{xray,c}}^{R/r_{xray,c}} x \sqrt{x^2 - (r/r_{xray,c})^2} \frac{3+x^2}{(1+x^2)^2} dx,$$

and  $R$  is the physical radius of the cluster and will be taken to be  $R = 3$  Mpc in the actual computation. Our conclusion is unaffected by this choice.

We have computed the projected X-ray cluster mass  $m_{xray}$  interior to the position of each arclike image  $r_{arc}$  or the corresponding radius of each weak lensing measurement  $r_0$  for the 21/13 strong/weak lensing clusters of known temperatures listed in Table 1 and Table 2, and the resulting  $m_{xray}$  versus  $m_{lens}$  are plotted in Fig.4 for  $\beta_{fit} = 2/3$  and a mean core radius of  $\langle r_{xray,c} \rangle = 0.25$  Mpc. It turns out that although both the strong and weak lensing determined cluster masses  $m_{lens,arc}$  and  $m_{lens,weak}$  show a good correlation with the X-ray masses  $m_{xray}$ , their amplitudes are very different:  $m_{lens,arc}/m_{xray} = 3.23 \pm 1.21$  and  $m_{lens,weak}/m_{xray} = 0.97 \pm 0.44$ . The scatter in the fit of  $m_{lens,weak}/m_{xray}$  can be reduced when cluster A2163 is excluded (Fig.4b) (Note that A2163 is one of the hottest clusters known so far). That is to say, there is a significant discrepancy between the strong lensing derived cluster masses and the X-ray cluster masses, while an excellent agreement between the weak lensing results and the X-ray masses is found. The only way to reconcile  $m_{lens,arc}$  with  $m_{xray}$  is to adopt a considerably small core radius for the gas profile. Fig.5 demonstrates another plot of  $m_{lens}$  against  $m_{xray}$  by reducing  $r_{xray,c}$  to 0.025 Mpc. In this case, the ratios of  $m_{lens,arc}$  and  $m_{lens,weak}$  to  $m_{xray}$  read  $1.42 \pm 0.87$  and  $0.91 \pm 0.35$ , respectively. Yet, this does not relax the disagreement between  $m_{lens,arc}$  and  $m_{lens,weak}$ . Rather, the employment of a smaller core radius leads to a significant increase of the X-ray cluster mass estimate at small radius.

Recall that the crucial point behind the remarkable agreement of the strong lensing and X-ray determined masses for the cooling flow clusters reported by Allen (1998) is the small core radii of  $r_{xray,c} \approx 40\text{--}75$  kpc, in contrast to  $r_{xray,c} \approx 250$  kpc for the non-cooling flow clusters.

### 3.3 Velocity dispersion of galaxies as the tracer of cluster potential

If galaxies trace the underlying gravitational potential of cluster, their velocity dispersion  $\sigma_{gal}$  would be a good indicator of dark matter. A strict way to derive the dynamical mass of cluster from the distributions of galaxy population and their velocity dispersion is to work with the Jeans equation. Here, we utilize an alternative approach to the issue. We adopt the so-called softened isothermal sphere model with a core radius  $r_{dark,c}$  for the total mass distribution of cluster, which is characterized by the velocity dispersion of galaxies. The original motivation was to examine whether  $\sigma_{gal}$  provides a proper cluster mass estimate (Wu & Fang 1997). The projected cluster mass within radius  $r$  is simply

$$m_{opt}(< r) = \frac{\pi\sigma_{gal}^2}{G} \left( \sqrt{r^2 + r_{dark,c}^2} - r_{dark,c} \right). \quad (5)$$

There are 21/18 clusters in Table 1/2 whose velocity dispersions are observationally determined. We compute their total masses in terms of eq.(5) at the corresponding positions of arclike images or weak lensing measurements. We first adopt a core radius of  $r_{dark,c} = 0.25$  Mpc, in accord with the distributions of luminous matter (galaxies and gas) in cluster, and the resulting  $m_{opt}$  are shown in Fig.6. It turns out that the weak lensing determined cluster masses  $m_{lens,weak}$  are in fairly good agreement with  $m_{opt}$  despite of the large scatters:  $m_{lens,weak}/m_{opt} = 1.08 \pm 0.70$ , whereas the strong lensing results  $m_{lens,arc}$  depart apparently from the expectation of  $m_{lens,arc} = m_{opt}$  with  $m_{lens,arc}/m_{opt} = 6.07 \pm 3.98$ . Motivated by the argument that the dark matter profile is sharply peaked at the cluster center relative to the luminous matter distribution (e.g. Hammer 1991; Wu & Hammer 1993; Durret et al. 1994; etc), we also present in Fig.6 the results  $m_{opt}$  for a smaller core radius of  $r_{dark,c} = 0.025$  Mpc. This indeed reduces the difference between  $m_{lens,arc}$  and  $m_{opt}$ , but simultaneously breaks down the accordance of  $m_{lens,weak}$  and  $m_{opt}$ . The mean ratios of strong and weak lensing results to the isothermal sphere model determined cluster masses are now  $m_{lens,arc}/m_{opt} = 1.44 \pm 0.97$  and  $m_{lens,weak}/m_{opt} = 0.63 \pm 0.35$ , respectively. The scatter in  $m_{lens,weak}/m_{opt}$  can be significantly reduced if the data sets of A2163 and RXJ1716 are excluded.

A more reasonable way to estimate the dynamical mass of cluster in terms of velocity dispersion of galaxies is to employ the virial theorem:  $M_{vir} = 3\sigma_{gal}^2 r_v / G$ , which measures the total cluster mass enclosed within a sphere of the so-called virial radius  $r_v$ . A direct comparison of the virial and lensing cluster masses is somewhat difficult because the virial radius  $r_v$  is usually much larger than the size which can be reached by the current gravitational lensing techniques. We display in Fig.7 the cluster masses given by strong/weak lensing and virial theorem for 10 clusters with the available data of  $M_{vir}$  in literature. The projected cluster mass derived from gravitational lensing would approach to the 3-D virial mass at radius as large as  $r_v$ . However, the fact that

the cluster regimes probed by the two methods show no overlaps can only lead us to arrive at the conclusion that these two independent methods seem to provide a consistent radial matter distribution of cluster.

## 4 DISCUSSION

### 4.1 Strong lensing: overestimates cluster mass ?

The consistence of the  $\sigma_{gal}\text{-}T$  relationship of the lensing clusters with  $\sigma_{gal} \propto T^{0.5}$  expected under the hypothesis of isothermal and hydrostatic equilibrium suggests that the gas and galaxies are good tracers of underlying gravitational potential of the clusters. Indeed, a number of recent studies have shown that clusters of galaxies suffer from little evolution, and their dynamical properties have remained almost unchanged since  $z \sim 0.8$  (Mushotzky, & Scharf 1977; Bahcall, Fan, & Cen 1997; Henry 1997; Rosati et al. 1998; Vikhlinin et al. 1988; etc.). This essentially justifies the employment of the Jeans equation for X-ray emitting gas in the lensing clusters at intermediate redshifts. On the other hand, the weak lensing probes the gravitational potential fields of the clusters in a completely different way. So, the excellent agreement between weak lensing and X-ray determined cluster masses serves as another convincing evidence for the lensing clusters being the dynamically relaxed systems.

A further examination of the mass determinations with eq.(1) tells us that there are no free parameters with which one can play when the redshifts of the lensing clusters and of the arclike images are observationally measured. It is unlikely that the replacement of the simple spherical lens model by a more sophisticated one can make a significant difference [see Allen (1998) for a detailed discussion; and references therein]. Therefore, we are forced to accept the fact that the present modeling of strong lensing event does provide a reliable cluster mass estimate.

However, from the comparisons of different cluster mass estimators in the above section, it is apparent that the cluster mass revealed by strong lensing exceeds that inferred from weak lensing and X-ray method by a factor of  $\sim 2 - 4$ . If we choose to trust the strong lensing result, we may need to break down the fairly good agreement between the weak lensing and X-ray derived cluster masses, and work out a mechanism which can account for the mass discrepancy between the strong lensing and the latter two methods. There are quite a number of mechanisms such as projection effect and asymmetrical mass distributions which may result in an overestimate of cluster mass from arclike images. But, these mechanisms will simultaneously influence the weak lensing results. In the following discussion we will focus on whether weak lensing and X-ray analysis give rise to an underestimate of the gravitating masses of clusters.

### 4.2 Weak lensing: underestimates cluster mass ?

In principle, the weak lensing method eq.(2) and (3) always provides a lower bound on the cluster mass  $m_{lens,weak}(< r_0)$  interior to radius  $r_0$ . So, the total mass within  $r_0$  could be considerably underestimated unless the outer control annulus  $r_{max}$  is set to be sufficiently large and/or the true

mass density profile drops sharply along outward radius. In the current measurements of weak lensing effects, a value of  $r_{max} \sim 1 - 2$  Mpc is often adopted due to the limited data coverages. If cluster exhibits rather a flat surface mass density, e.g. a power-law of  $\propto r^{-\gamma}$  with index  $\gamma < 1$ , it is not impossible that the true cluster masses can be underestimated by a factor of as large as  $\sim 2$ , according to the formalism of Kaiser et al. (1994):  $\bar{\sigma}/\zeta = (a^2 - 1)/(a^2 - a^{2-\gamma})$  where  $a = r_0/r_{max}$ .

Another crucial point is relevant to the application of weak lensing inversion technique to the central region of cluster close to the Einstein radius, where the actual comparison of strong lensing and weak lensing determined cluster masses becomes possible. However, because the giant arc traces approximately the Einstein radius and because the weak lensing method can be marginally applicable to such a small radius, large uncertainties could be introduced into the shear measurements within the positions of arcs/arclets (e.g. Seitz & Schneider 1995). This even does not account for the possible contamination of central cluster galaxies due to the small number of background faint galaxies near the Einstein radius. From Fig.2 it is easily recognized that the innermost radii of the weak lensing measurements are always larger than or equal to the arc radii. Therefore, one cannot exclude the possibility that the disagreement of the strong and weak inferred cluster masses arises simply from the inappropriate application of the weak lensing inversion technique to the central regimes of clusters, although it has been shown that the cluster mass is only slightly underestimated at the cluster center if a general method for the nonlinear cluster mass reconstruction is used (Kaiser 1995; Schneider & Seitz 1995; Seitz & Schneider 1995).

#### 4.3 X-ray analysis: underestimates cluster mass ?

An accurate estimate of cluster mass from the X-ray measurement depends on our understanding of the gas distribution and its dynamical state in cluster, which is closely connected to how significant the X-ray emitting gas deviates from the state of hydrostatic equipartition with the gravitational potential of the whole cluster. This argument is twofold: (1)The complex dynamical activities in cluster may only take place locally and on small scales such as the substructure merging and irregular temperature patterns, while the cluster as a whole can be regarded as a violently relaxed system; (2)Cluster is still in forming stage and thereby, cannot be modeled as a virialized system at all.

In the first circumstance, the Jeans equation may be safely applied to large radius but fails at small scales. Such a dynamical model can account for the excellent agreement between weak lensing and X-ray cluster masses at relatively large radius, and the mass discrepancy between X-ray and strong lensing measurements within the central cores of clusters. Further evidences for this scenario come from the overall  $\sigma_{gal}-T$  relationship for the lensing clusters (Fig.1) and the recent observations of cluster abundances and other dynamical properties at redshift out to  $z \sim 0.8$  (Mushotzky, & Scharf 1997; Bahcall et al. 1997; Rosati et al. 1998; etc.), i.e., the significant cosmic and dynamical evolutions do not play a dominant role for clusters of galaxies as a whole since  $z \sim 0.8$ . There are a number of mechanisms that could affect the determinations of cluster masses on small scales based

on the X-ray observations, among which the presence or lack of the cooling flows inside the cores of clusters is likely to be the major source of uncertainties (Allen 1998). If the core radius of the X-ray emitting gas profile is overestimated due to the contamination of these central dynamical activities, we can indeed reconcile the strong lensing determined cluster masses with the X-ray measurements by substantially reducing the X-ray core radius (Fig.5). Recent analyses by Markevitch (1997) and Girardi et al. (1997b) for A1689 and A2218, based on the high resolution X-ray/optical images, have revealed that the local dynamical activities like the ongoing subcluster mergers in the core regions probably make the hydrostatic mass estimate inapplicable. Additional supports come from the numerical simulations of cluster formation and evolution. For instances, Bartelmann & Steinmetz (1996) showed that utilizing a  $\beta$  model for a dynamical active cluster may lead to an average underestimate of the true cluster mass by a factor of  $\sim 40\%$ , and strong lensing preferentially selects clusters that are dynamically more active than the average. From an extensive analysis of the  $\beta$  model as a cluster mass estimator, Evrard, Metzler & Navarro (1996) concluded that while the mass estimates based on the hydrostatic, isothermal  $\beta$  model are remarkably accurate, the ratio of the estimated cluster mass in terms of the  $\beta$  model to the true cluster mass increases with increasing radius, with the true cluster mass being underestimated by the  $\beta$  model toward cluster center when  $\Omega_0 = 1$ , and merging rates are increased at low redshift. This is fairly consistent with our speculation (1).

The second possibility is of interest when a large  $\Omega_m$  universe (e.g.  $\Omega_m = 1$ ) is preferred, in which clusters of galaxies formed very recently and may still be in a stage of dramatic dynamical evolution. This may essentially invalidate the application of the Jeans equation without considering the infall motions of the materials inside and around the clusters. The coincidence between the weak lensing and X-ray determined cluster masses (see Fig.4) does not ensure that both methods would not result in an underestimate of total cluster masses. It is somewhat unfortunate if we have to accept this scenario, though there have been no convincing observations so far to confirm this argument.

#### 4.4 Velocity dispersion of galaxies: a good indicator of cluster ?

Unlike the diffuse X-ray gas, cluster galaxies are unaffected by the presence of the (non)cooling flows and the nonthermal pressure such as magnetic field and therefore, are probably a better indicator of mass distributions of clusters. However, a precise measurement of the galaxy velocity dispersion to large radius from the cluster center is difficult. Employment of the Jeans equation for galaxies among the ensemble clusters including lensing ones at intermediate redshifts have become possible only recently (Carlberg, Yee, & Ellingson 1997). On the other hand, the virial and lensing cluster masses are basically consistent with each other (see Fig.7), though the two methods probe very different regions of clusters.

Attempts have been made to fit the lensing derived mass profile with either a singular or softened isothermal sphere model for many individual lensing clusters (e.g. Fahlman et al. 1994; Tyson & Fischer 1995; Squires et al. 1997a,b;

Luppino & Kaiser 1997; Fischer & Tyson 1998; Tyson, Kochanski, & Dell’Antonio 1998; etc), which have nevertheless yielded a controversial result. From our statistical study (see Fig.6), an uncomfortably small core radius of  $\sim 0$  may be required for an isothermal dark matter distribution if the strong lensing data alone are used, while the weak lensing results allow the core size of dark matter profile to be as large as the one for luminous matter distributions. A combination of the strong and weak lensing analyses suggests that an isothermal sphere model with a compact but non-zero core and characterized by the observed velocity dispersion of galaxies  $\sigma_{gal}$  is likely to provide a good description of total mass distribution of cluster. This is consistent with the first high resolution mass map of CL0024+1654 through parameter inversion of the multiple images of a background galaxy (Tyson et al. 1998), which has detected the presence of a soft core of  $\sim 0.066$  Mpc. Alternatively, if the true mass distribution of cluster is close to an isothermal sphere model, the statistical agreement of the lensing measured cluster masses with those expected from the isothermal model indicates that there is no strong bias between the velocity of the dark matter particles and of the galaxies. In other words, velocity dispersion of galaxies seems to be a good indicator of the gravitating mass of cluster.

## 5 CONCLUSIONS

Statistical comparisons of different mass estimators among lensing clusters based on the published data in literature have revealed the following features: (1) Strong gravitational lensing, which is believed to be the most reliable mass estimator, gives rise to a systematically larger projected cluster within the position of arclike image than those derived from the weak lensing technique and the X-ray measurements; (2) There is an excellent agreement between the weak lensing and X-ray derived cluster masses; (3) An isothermal sphere with a compact core radius, which is characterized by the velocity dispersion of galaxies, provides a good description of total mass distribution of cluster.

It is possible to reconcile the different cluster mass estimators under the following way: both the weak lensing technique and the X-ray measurements based on the hydrostatic equilibrium hypothesis are inappropriate to probe the matter distributions in the central regions of clusters, which may underestimate the gravitating masses enclosed within the cluster cores by a factor of 2–4 as compared with the strong lensing method. Nevertheless, these cluster mass estimators may be safely applied on large scales outside the core radius, which is supported by the studies of dynamical properties of clusters and also the excellent agreement between the weak lensing and X-ray measured cluster masses. Basically, a smaller core radius of  $r_{dark,c} \sim$  a few ten kpc is needed for both dark and luminous matter profiles in order to explain the detected mass discrepancy. Very likely, it is the local dynamical activities that lead the dark matter profile to appear more peaked than the luminous matter distributions at the centers of clusters. Overall, the light profile traces the dark matter distribution in cluster, and the velocity dispersion of galaxies and the temperature of gas are both good indicators of the underlying gravitational potentials of the whole clusters.

The cosmological implications of this work are as follows: The mass-to-light ratio  $M/L$  and the baryon fraction  $f_b$  revealed by the current optical and X-ray observations of clusters are indeed reliable indicators for the overall matter composition of clusters and thereby the universe, though these quantities may have rather a large uncertainty on small scales of  $\sim 100$  kpc. As a result, we have to accept a low mass density universe of  $\Omega_m \approx 0.1-0.4$ , as suggested by the two independent measurements of the cluster matter compositions, the ratio  $M/L$  [(dark+luminous)/luminous] (e.g. Bahcall, Lubin, & Dorman, 1995) and the baryon fraction  $f_b$  [baryon/(baryon+nonbaryon)] (e.g. White et al. 1993). If so, we should be aware that the fraction of baryonic matter in the universe is not small at all:  $\sim 20-30\%$  of the matter in the universe is luckily visible !

## ACKNOWLEDGMENTS

We gratefully acknowledge the referee, Vincent Eke, for valuable comments and suggestions. This work was supported by the National Science Council of Taiwan, under Grant No. NSC87-2816-M008-010L and NSC87-2112-M008-009, and the National Science Foundation of China, under Grant No. 1972531.

## REFERENCES

- Allen S.W., 1998, MNRAS, 296, 392  
 Allen S.W., Fabian A.C., Kneib J.P., 1996, MNRAS, 279, 615  
 Bahcall N.A., Fan X., Cen R., 1997, ApJ, 485, L53  
 Bahcall N.A., Lubin L.M., Dorman V., 1995, ApJ, 447, L81  
 Bartelmann M., Steinmetz M., 1996, MNRAS, 283, 431  
 Bonnet H., Mellier Y., Fort B., 1994, ApJ, 427, 83  
 Bower R.G., Smail L., 1997, MNRAS, 290, 292  
 Campusano L.E., Kneib J.-P., Hardy E., 1998, ApJ, 496, L79  
 Carlberg R.G., Yee H.K.C., Ellingson E., 1997, ApJ, 478, 462  
 Carlberg R.G., Yee H.K.C., Ellingson E., Abraham R., Gravel P., Morris S., Pritchet C.J., 1996, ApJ, 462, 32  
 Cavaliere A., Fusco-Femiano R., 1976, A&A, 49, 137  
 Clowe D., Luppino G.A., Kaiser N., Henry J.P., Gioia I.M., 1998, ApJ, submitted (astro-ph/9801208)  
 Durret F., Gerbal D., Lachièze-Rey M., Lima-Neto G., Sadat R., 1994, A&A, 287, 733  
 Ebbels T., Ellis R., Kneib J.-P., Le Borgne J.-F., Pelló R., Smail I., Sanahuja, B., 1998, MNRAS, 295, 75  
 Ensslin T.A., Biermann P.L., Kronberg P.P., Wu X.-P. 1997, ApJ, 477, 560  
 Evrard A. E., Metzler C. A., Navarro J. F., 1996, ApJ, 469, 494  
 Fahlman G., Kaiser N., Squires G., Woods D., 1994, ApJ, 437, 56  
 Fischer P., Tyson J.A., 1997b, AJ, 114, 14  
 Fischer P., Bernstein G., Rhee G., Tyson J.A. 1997a, AJ, 113, 521  
 Fort B., Mellier Y., 1994, A&AR, 5, 239  
 Girardi M., Fadda D., Giuricin G, Mardirossian F., Mezzetti M., 1996, ApJ, 457, 61  
 Girardi M., Fadda D., Escalera E., Giuricin G, Mardirossian F., Mezzetti M., 1997b, ApJ, 490, 56  
 Girardi M., Escalera E., Fadda D., Giuricin G, Mardirossian F., Mezzetti M., 1997a, ApJ, 482, 41  
 Hammer F., 1991, ApJ, 383, 66  
 Henry J.P., 1997, ApJ, 489, L1  
 Henry J.P., Briel U.G., 1995, ApJ, 443, L9  
 Hoekstra H., Franx M., Kuijken K., Squires G., 1998, ApJ, in press



- Kaiser N., 1995, *ApJ*, 439, L1
- Kaiser N., Squires G., 1993, *ApJ*, 404, 441
- Kaiser N., Squires G., Fahlman, G., Woods D., 1994, in Proc. of 1994 Herstmonceux conference “Wide Field Spectroscopy” (astro-ph/9411029)
- Kneib J.P., Soucail G., 1995, in *Astrophysical Applications of Gravitational Lensing*, C.S.Kochanek and J.N.Hewitt (eds.), Kluwer Academic Publishers, p.113
- Le Fevre O., Hammer F., Angonin M.C., Gioia I.M., Luppino G.A., 1994, *ApJ*, 324, L1
- Loeb A., Mao S., 1994, *ApJ*, 435, L109
- Luppino G.A., Kaiser N., 1997, 475, 20
- Markevitch M., 1996, *ApJ*, 465, L1
- Markevitch M., 1997, *ApJ*, 483, L17
- Miralda-Escudé J., Babul A., 1995, *ApJ*, 449, 18
- Mushotzky R.F., Scharf C.A., 1997, *ApJ*, 482, L13
- Ostriker J.P., Steinhardt P.J., 1995, *Nature*, 377, 600
- Rosati P., Ceca R.D., Norman C., Giacconi R., 1998, *ApJ*, 492, L21
- Schneider P., Seitz, C., 1995, *A&A*, 294, 411
- Seitz C., Kneib J.-P., Schneider P., Seitz S., 1996, *A&A*, 314, 707
- Seitz & Schneider P., 1995, *A&A*, 297, 287
- Smail I., Dickinson M., 1995 *ApJ*, 455, L99
- Smail I., Ellis R.S., Dressler A., Couch W.J., Oemler A., Jr. Sharples R.M., Butcher H., 1997, *ApJ*, 479, 70
- Squires G., Kaiser N., Babul A., Fahlman G., Woods D., Neumann D.M., Böhringer H., 1996, *ApJ*, 461, 572
- Squires G., Kaiser N., Fahlman G., Babul A., Woods D., 1997a, *ApJ*, 469, 73
- Squires G., Neumann D.M., Kaiser N., Arnaud M., Babul A., Böhringer H., Fahlman G., Woods D., 1997b, *ApJ*, 482, 648
- Smail I., Ellis R.S., Dressler A., Couch W.J., Oemler A., Jr. Sharples R.M., Butcher H., 1997, *ApJ*, 479, 70
- Taylor A.N., Dye S., Broadhurst T.J., Benitez N., van Kampen E., 1998, *ApJ*, submitted
- Tyson J.A., Kochanski G.P., Dell’Antonio I.P., 1998, *ApJ*, submitted
- Tyson J.A., Fischer P., 1995, *ApJ*, 446, L55
- Vikhlinin A., McNamara B.R., Forman W., Jones C., Quintana H., Hornstrup A., 1998, *ApJ*, 498, L21
- White S.D.M., Navarro J.F., Evrard A.E., Frenk C.S., 1993, *Nature*, 366, 429
- Wu X.-P., 1994, *ApJ*, 436, L115
- Wu X.-P., Fang L.-Z., 1996a, *ApJ*, 461, L5
- Wu X.-P., Fang L.-Z., 1996b, *ApJ*, 467, L45
- Wu X.-P., Fang L.-Z., 1997, *ApJ*, 483, 62
- Wu X.-P., Hammer F., 1993, *MNRAS*, 262, 187
- Wu X.-P., Hammer F., 1995, *A&A*, 299, 353

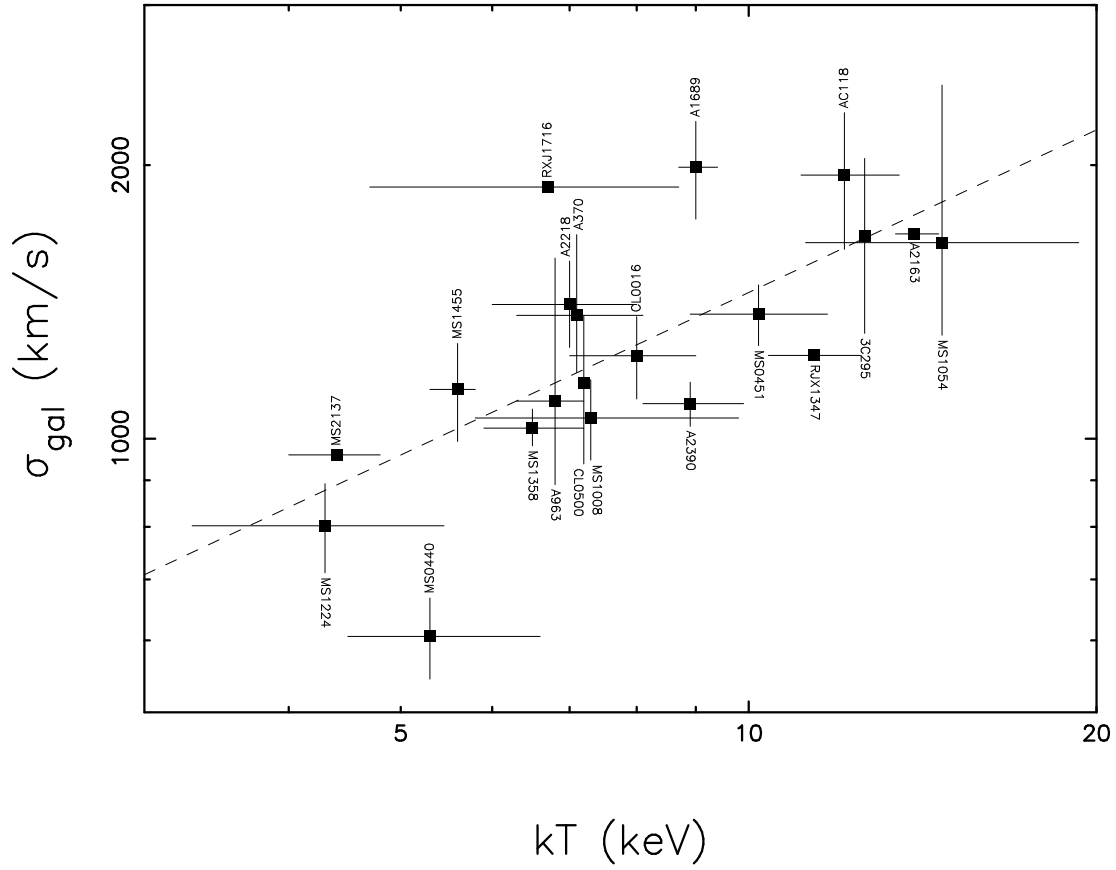


**Figure 1.** The  $\sigma_{gal}$ - $T$  relationship of the 20 lensing clusters in Table 1 and Table 2, for which both velocity dispersion  $\sigma_{gal}$  and temperature  $T$  are observationally determined. The dashed line is the best-fit to the data:  $(\sigma_{gal}/\text{km s}^{-1}) = 10^{2.57 \pm 0.13} (kT/\text{keV})^{0.59 \pm 0.14}$ .

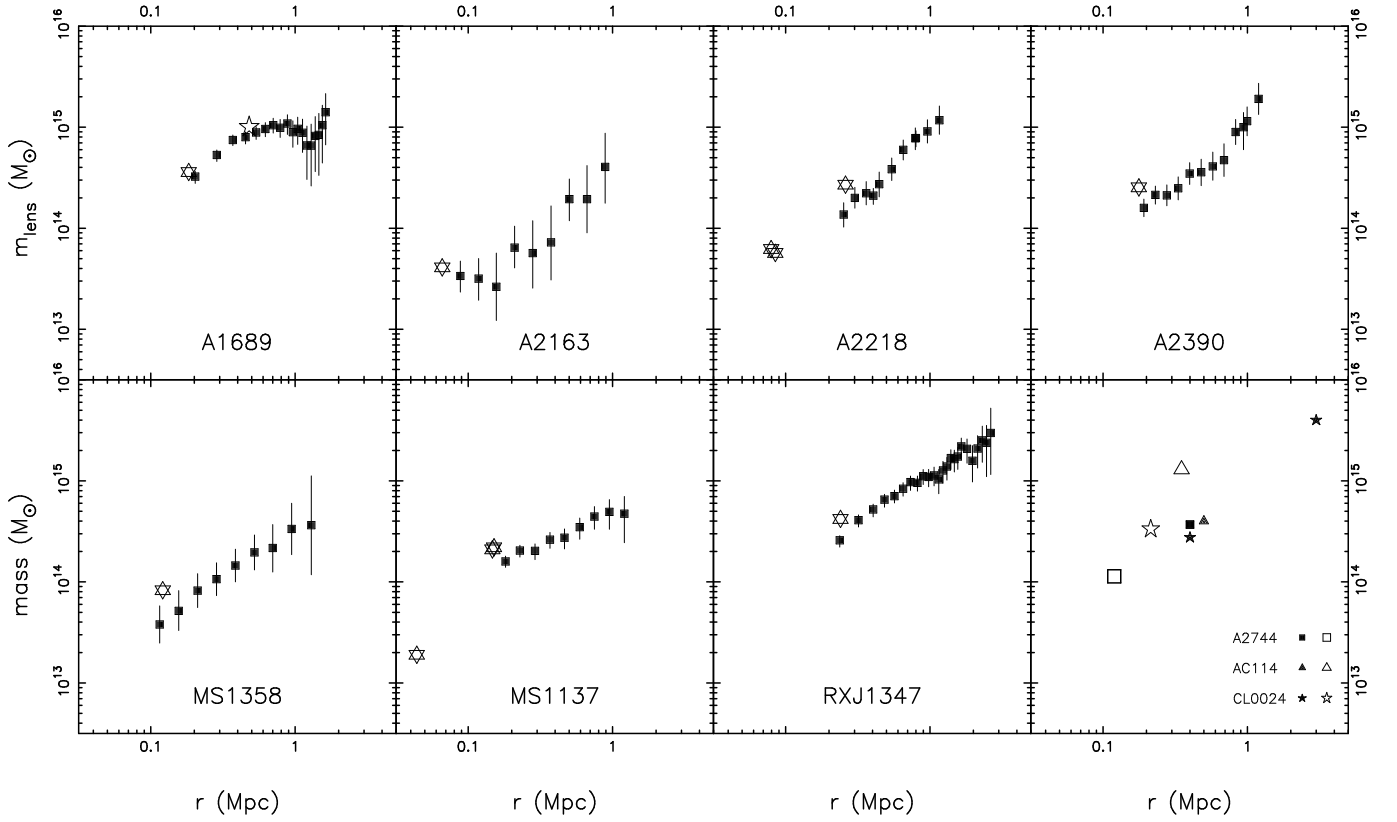


**Figure 2.** Comparison of the strong and weak lensing determined cluster masses among individual clusters. The open and filled symbols represent the strong and weak lensing results, respectively. Note that the giant arc was used for the calibration of the weak lensing measurements in A1689, for which we have also displayed the recent result (open asterisk) obtained from the measurement of the deficit of red galaxy population behind A1689 for comparison (Taylor et al. 1998). The uncertainties of the strong lensing results are not shown, which turn to be quite small when the positions and redshifts of the arcs are observationally determined.

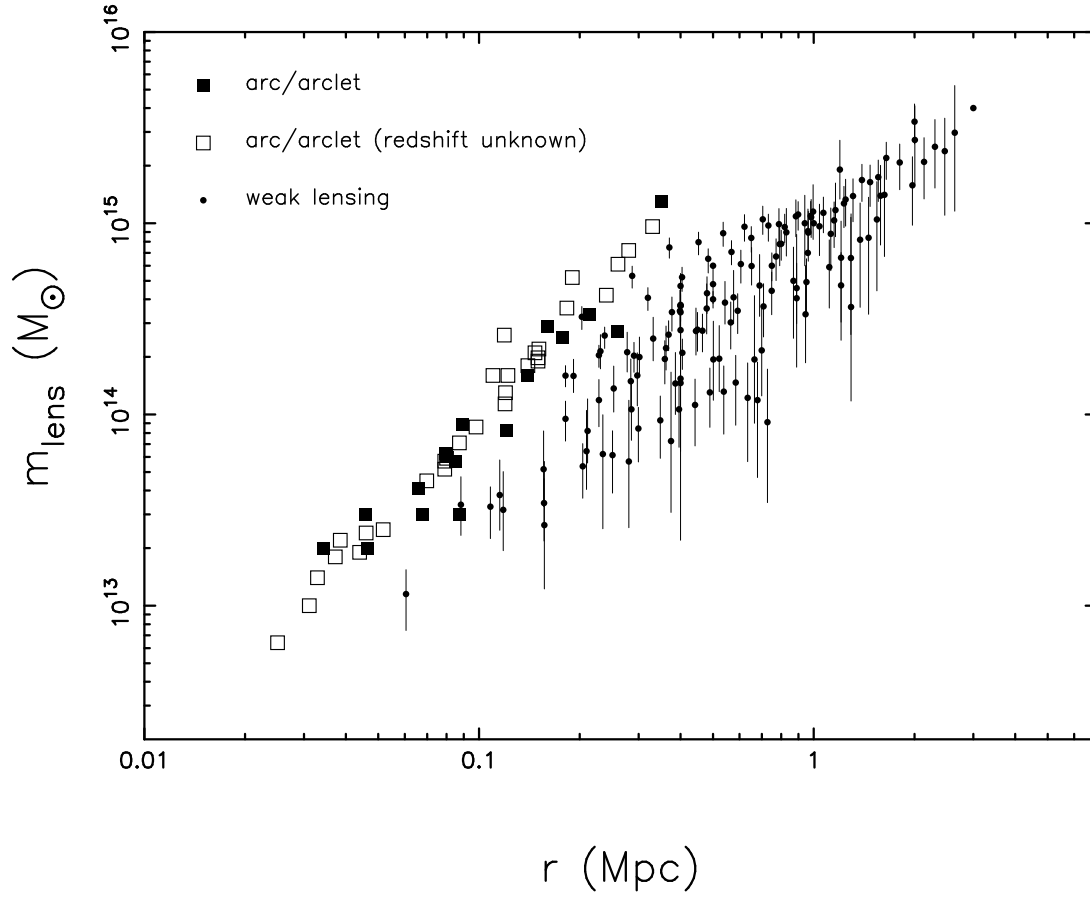


**Figure 3.** The strong and weak lensing measured cluster masses are plotted against the cluster radii for all the data sets in Table 1 and Table 2. It appears that the gravitating masses revealed by the arclike images systematically exceed those derived from the inversion of the weakly distorted images of background galaxies around clusters.

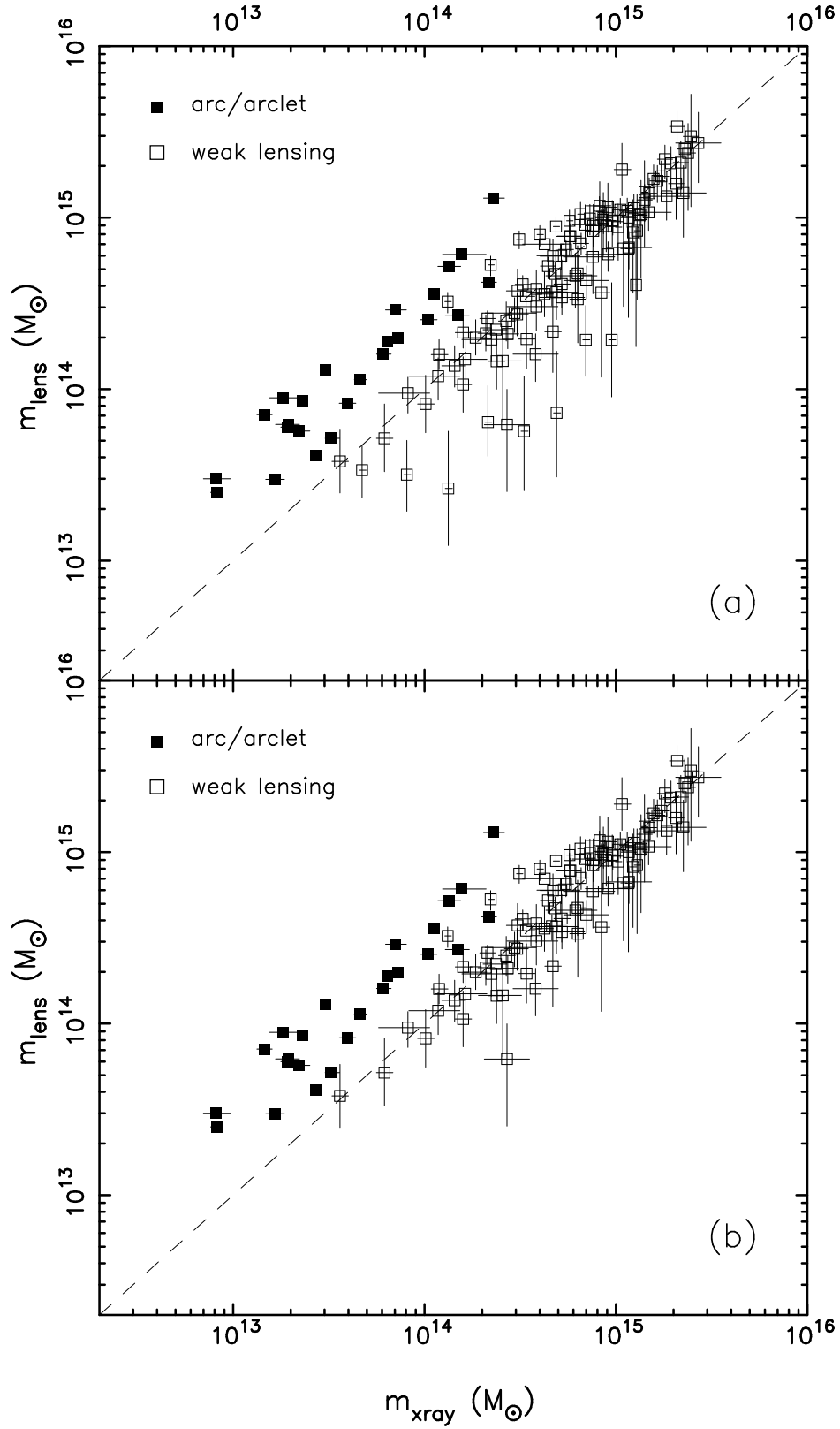


**Figure 4.** Gravitational lensing determined cluster masses  $m_{lens}$  versus the hydrostatic masses  $m_{xray}$  given by the X-ray diffuse gas. Only those clusters in Table 1 and Table 2 whose temperatures are spectroscopically measured are shown. A conventional isothermal  $\beta$  model with  $\beta_{fit} = 2/3$  and core radius  $r_{xray,c} = 0.25$  Mpc is adopted for the gas distribution. It is remarkable that  $m_{xray}$  agree essentially with the weak lensing results (a), while an excellent agreement is reached when cluster A2163 is excluded (b). The horizontal error bars only reflect the uncertainties in the measurements of temperature. The dashed line is not a fit to the data but assumed that  $m_{lens} = m_{xray}$ .

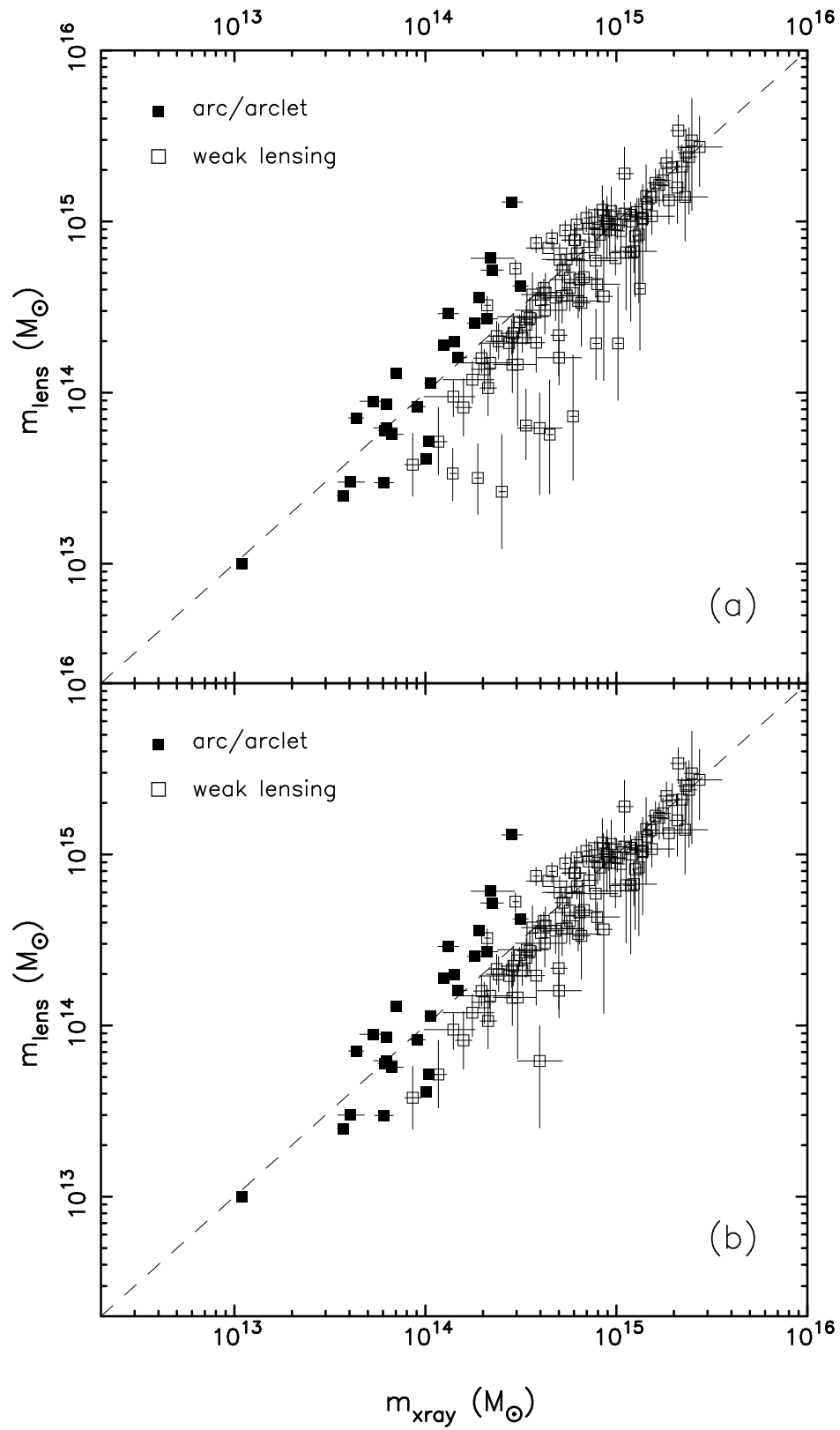


**Figure 5.** The same as Fig.4 but for a much smaller core radius of  $r_{\text{xray},c} = 0.025$  Mpc in the gas profile.

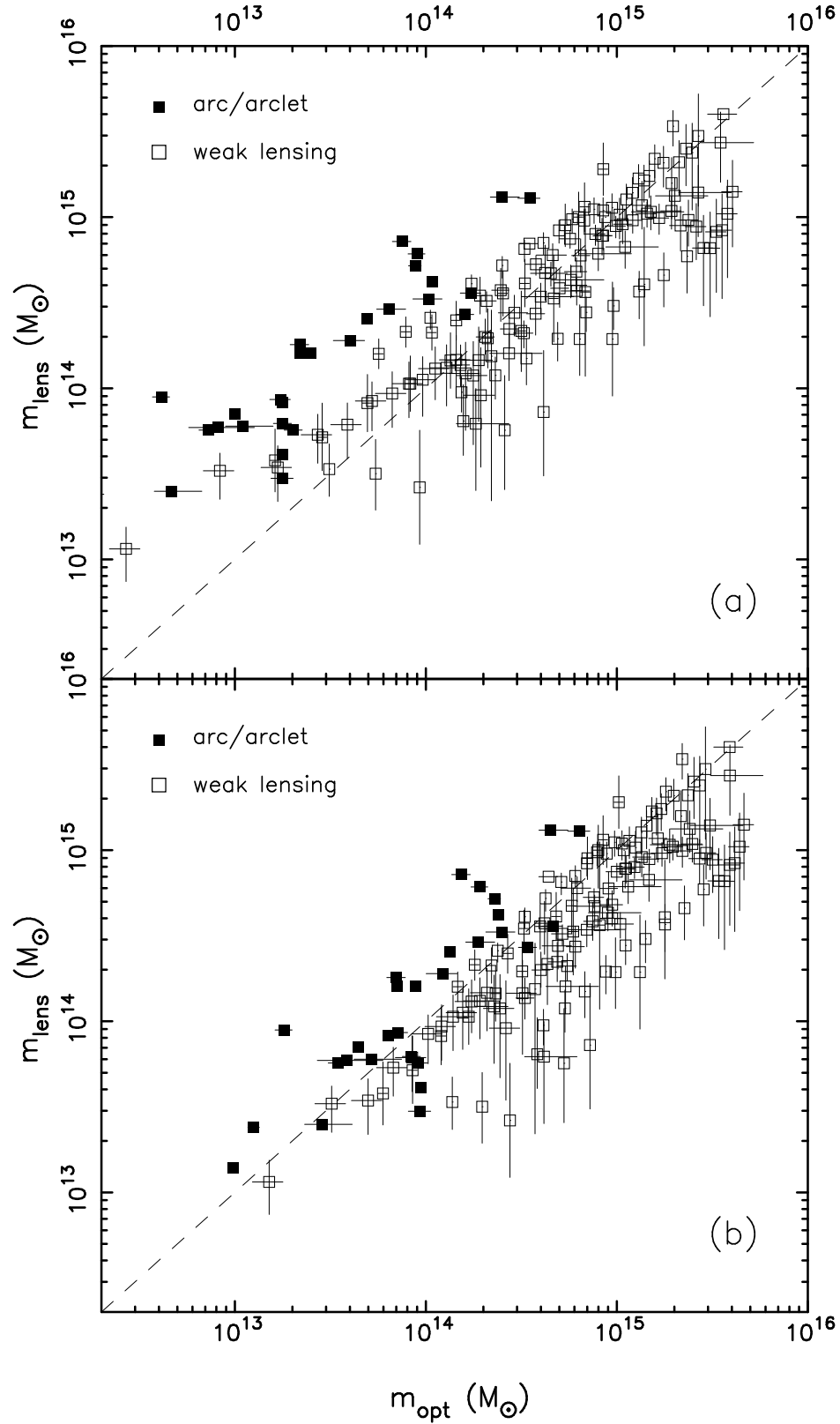


**Figure 6.** Gravitational lensing determined cluster masses  $m_{lens}$  are plotted against the theoretically expected results  $m_{opt}$  from a softened isothermal sphere model for the total mass distributions of clusters, which is characterized by the velocity dispersion  $\sigma_{gal}$  of galaxies and a core radius  $r_{dark,c}$ . (a)  $r_{dark,c} = 0.25$  Mpc and (b)  $r_{dark,c} = 0.025$  Mpc. Only the clusters whose  $\sigma_{gal}$  are observationally measured are shown, and the horizontal error bars represent the uncertainties in  $\sigma_{gal}$ . The dashed line is not a fit to the data but assumed that  $m_{lens} = m_{opt}$ . The dispersions in  $m_{lens}$  can be considerably reduced if the weak lensing data of A2163 and RXJ1716 are excluded.

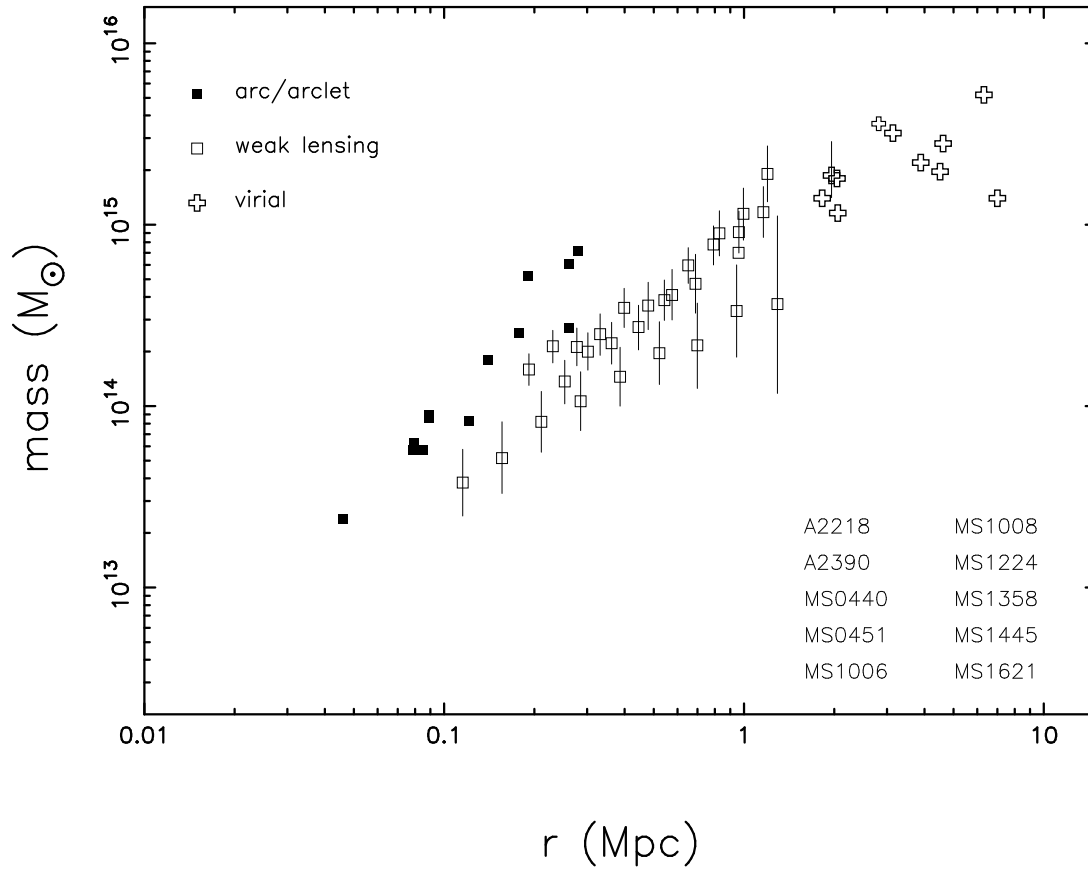


**Figure 7.** A comparison of the cluster masses derived from gravitational lensing and virial theorem. At sufficiently large radius, the deviation of the projected masses from the spatial (virial) values should become negligible. According to the present data sets, it is unlikely that there are significant differences between the two mass estimators. The virial masses are from Carlberg et al. (1996) and Girardi et al. (1997a).